Science Advances

AAAS

advances.sciencemag.org/cgi/content/full/3/10/eaao4204/DC1

Supplementary Materials for

Enhanced mobility $CsPbI_3$ quantum dot arrays for record-efficiency, high-voltage photovoltaic cells

Erin M. Sanehira, Ashley R. Marshall, Jeffrey A. Christians, Steven P. Harvey, Peter N. Ciesielski, Lance M. Wheeler, Philip Schulz, Lih Y. Lin, Matthew C. Beard, Joseph M. Luther

Published 27 October 2017, *Sci. Adv.* **3**, eaao4204 (2017)
DOI: 10.1126/sciadv.aao4204

This PDF file includes:

- Supplementary Materials and Methods
- fig. S1. Performance of FAI-coated and control devices.
- fig. S2. Light absorption following FAI posttreatment.
- fig. S3. Comparison of EQE with AX posttreatment.
- fig. S4. Reproducibility of FAI-coated $CsPbI_3$ QD device performance.
- fig. S5. XPS spectroscopy.
- fig. S6. FTIR spectra of $CsPbI_3$ QDs.
- fig. S7. Crystal structure of $CsPbI_3$ QDs.
- fig. S8. $CsPbI_3$ QD film morphology.
- fig. S9. Comparison of terahertz $\mu_s \times \tau$ product.
- fig. S10. PL lifetime of $CsPbI_3$.
- Reference (*34*)

Supplementary Materials and Methods

X-ray photoemission spectroscopy. XPS data was taken on a Kratos NOVA spectrometer calibrated to the Fermi edge and core level positions of sputter-cleaned metal (Au, Ag, Cu, Mo) surfaces. Spectra were acquired using monochromated Al Kα radiation (1486.7 eV) at a resolution of 600 meV (pass energy 20 eV). The data was averaged from multiple spots on the sample while the X-ray intensity was held low (15 W anode power) to avoid sample degradation (*34*) and fit using Pseudo-Voigt profiles.

Scanning electron microscopy. Samples were mounted on aluminum stubs with double-sided carbon tape and sputter-coated with 3 nm of Iridium prior to imaging. Images were obtained with a FEI Quanta 400 FEG instrument (FEI, Hillsboro, OR). Imaging was performed with a beam accelerating voltages of 30 keV.

Time-resolved photoluminescence. Time resolved photoluminescence was measured using a Hamamatsu streak camera system (C10910-05), while the excitation source was a Fianium Supercontinuum high power broadband fiber laser (SC400-2-PP). The chosen excitation wavelength was 530 nm at ~25 μW power on a spot size of 0.02 mm^2.

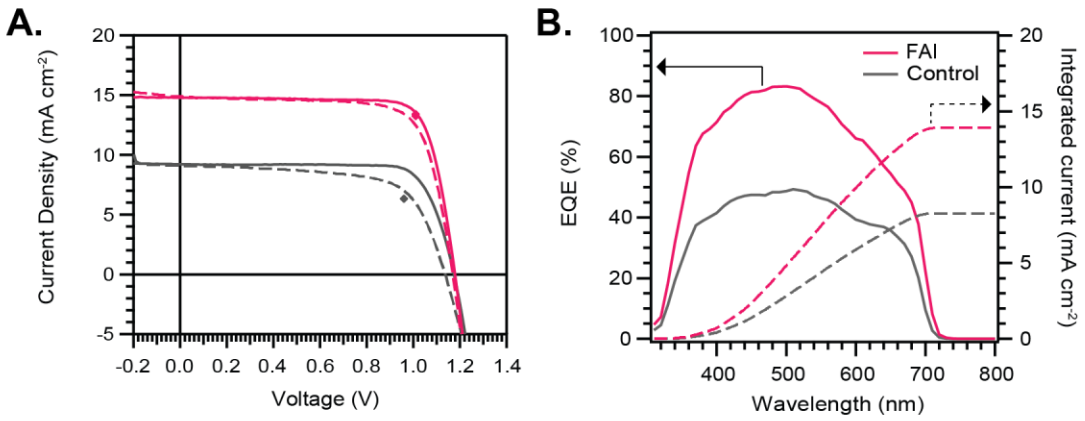

fig. S1. Performance of FAI-coated and control devices. (**A**) *J-V* scans in the forward (dotted) and reverse (solid) directions for FAI-coated (pink) and control (grey) devices. The SPO for each device is indicated by the diamond marker. (**B**) EQE (solid) and integrated current (dotted) for the FAI-coated (pink) and control (grey) devices.

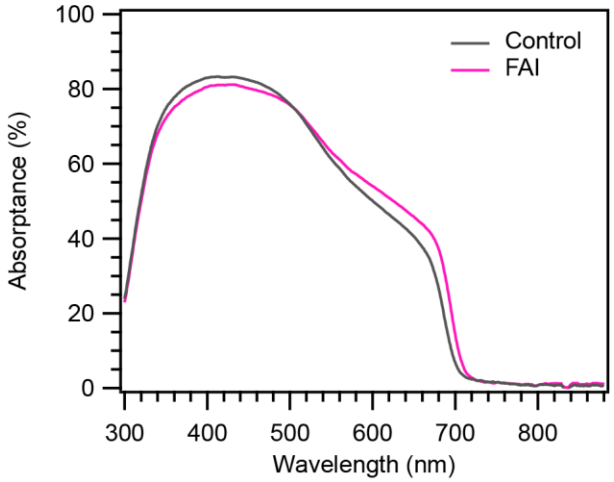

fig. S2. Light absorption following FAI posttreatment. Absorptance spectra of $CsPbI_3$ QD films on glass with (pink) and without (grey) the FAI post-treatment.

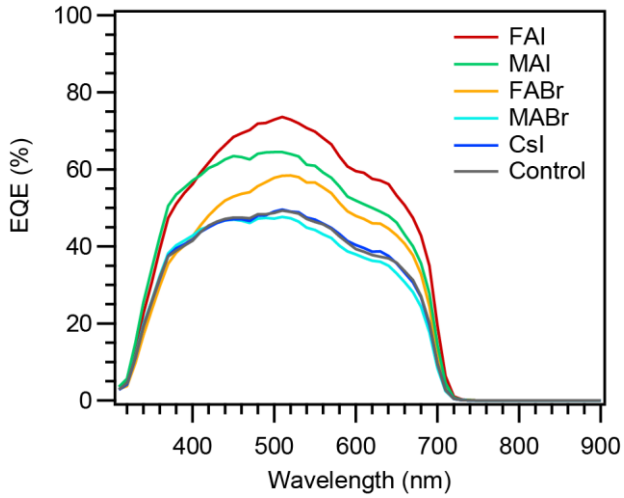

fig. S3. Comparison of EQE with AX posttreatment. EQE of devices treated with different AX salts observe similar EQE onset at ~700 nm.

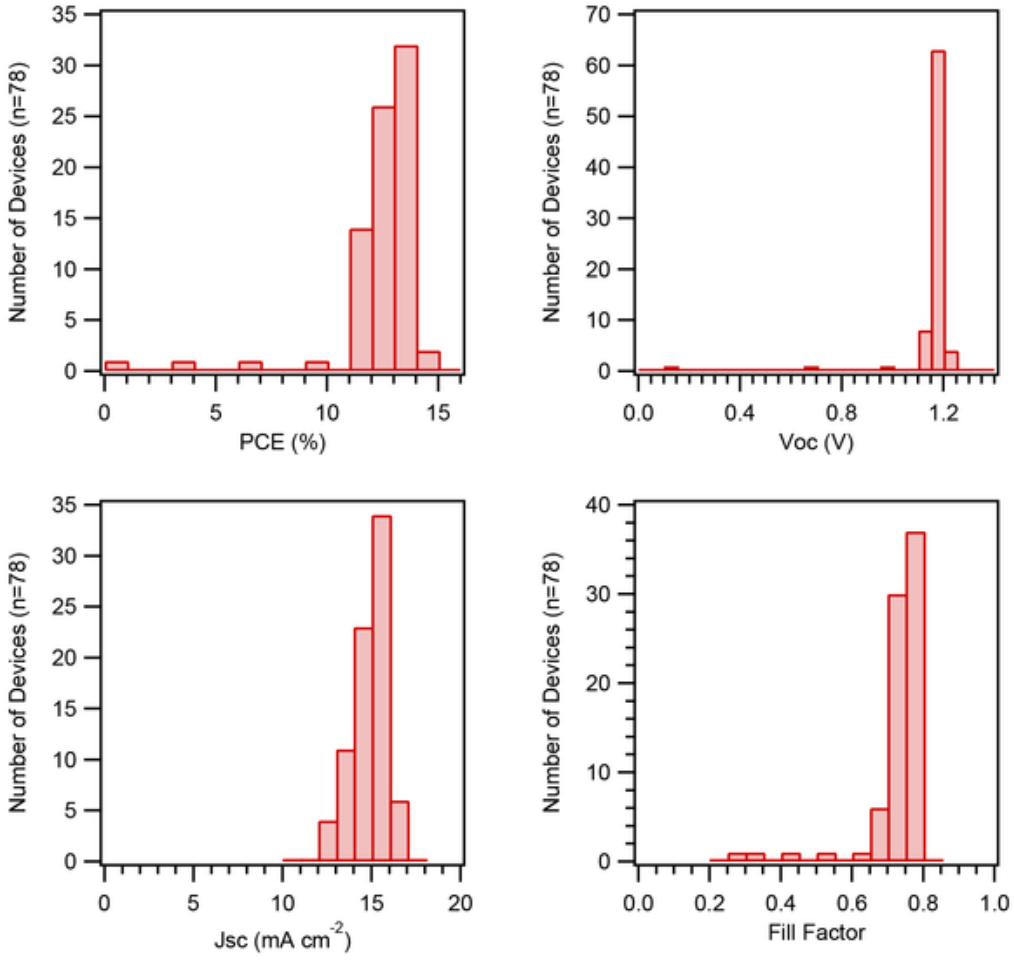

fig. S4. Reproducibility of FAI-coated $CsPbI_3$ QD device performance. Histograms of the PCE, V_{OC}, J_{SC} and FF of FAI-coated $CsPbI_3$ QD devices (n=78).

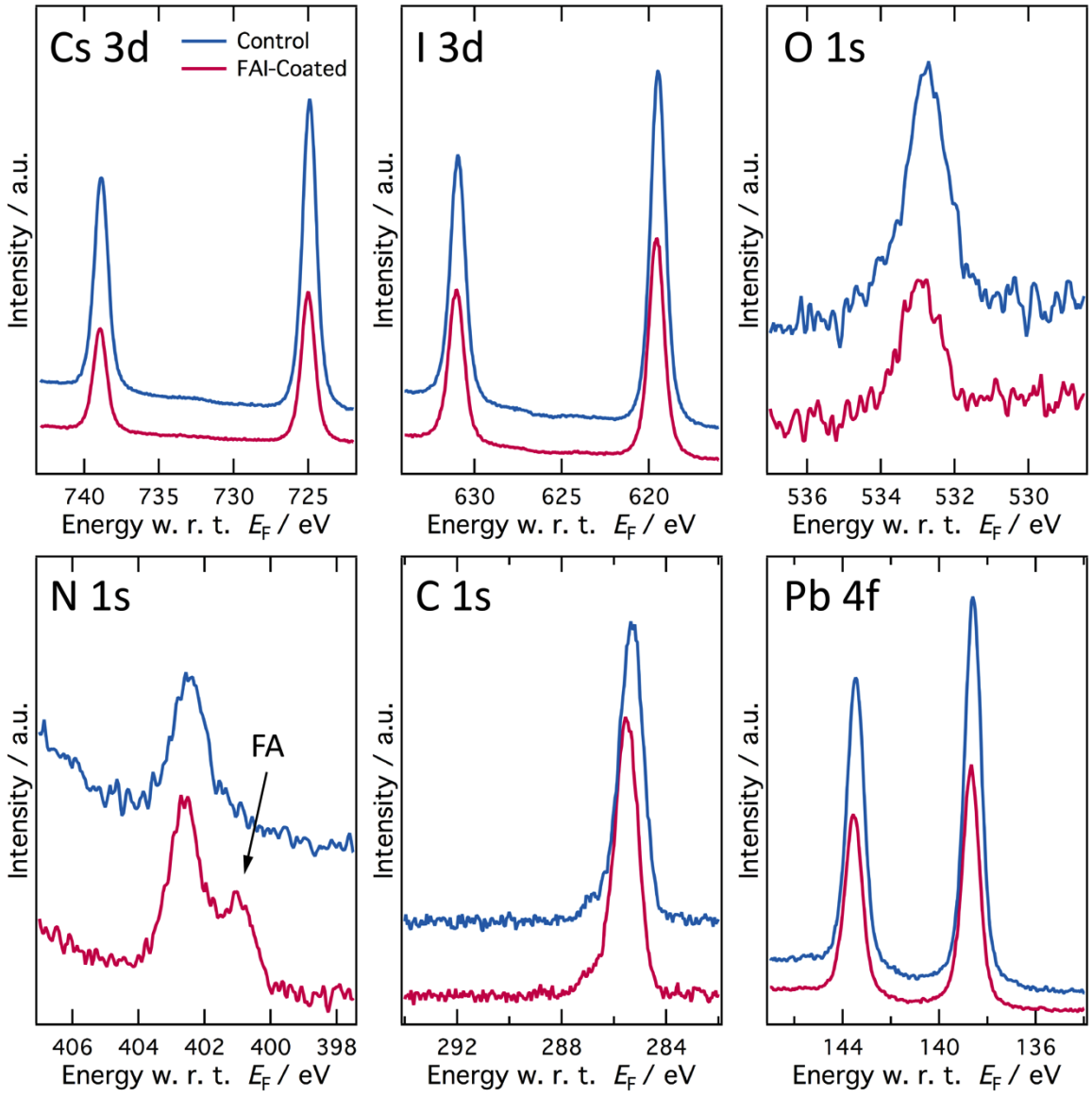

fig. S5. XPS spectroscopy. XPS core level spectra of $CsPbI_3$ QD films on TiO_2/FTO/glass. The presence of FA^+ species is observed by an additional peak centered at 401 eV binding energy in the N 1s core level region. Furthermore, the surface composition changes upon FAI treatment. The Cs^+:Pb^{2+} ratio drops from 0.91 to 0.74 indicating a decrease in Cs^+ content at the surface. At the same time, the I^-:Pb^{2+} ratio rises from 2.73 to 2.83 corroborating the results of the ToF-SIMS measurements. A decrease in the oxygen content upon FAI treatment indicates the further removal of residual oleate groups from the QD surface.

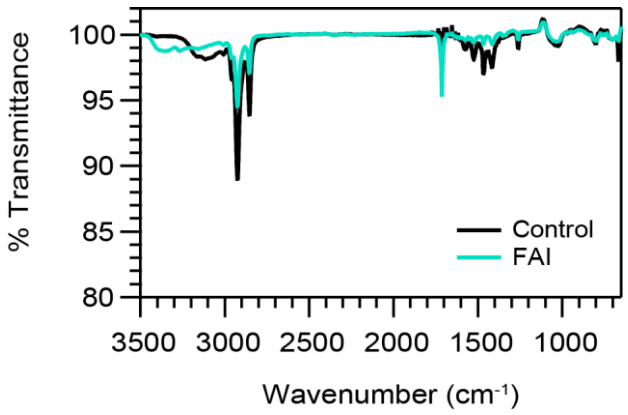

fig. S6. FTIR spectra of $CsPbI_3$ QDs. Fourier-transformed infrared (FTIR) spectra of $CsPbI_3$ QD films with (green) and without (black) FAI post-treatment. The emergence of the peak at 1712 cm^{-1} is indicative of the presence of FA.

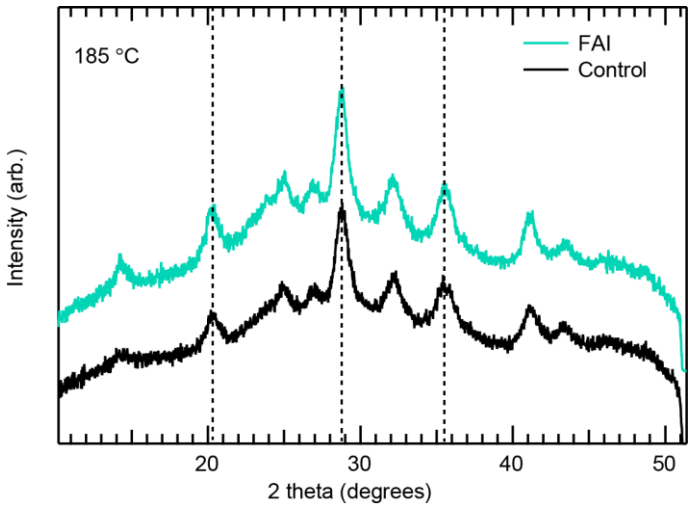

fig. S7. Crystal structure of $CsPbI_3$ QDs. X-ray diffraction pattern for $CsPbI_3$ QD films with (green) and without (black) FAI post-treatment.

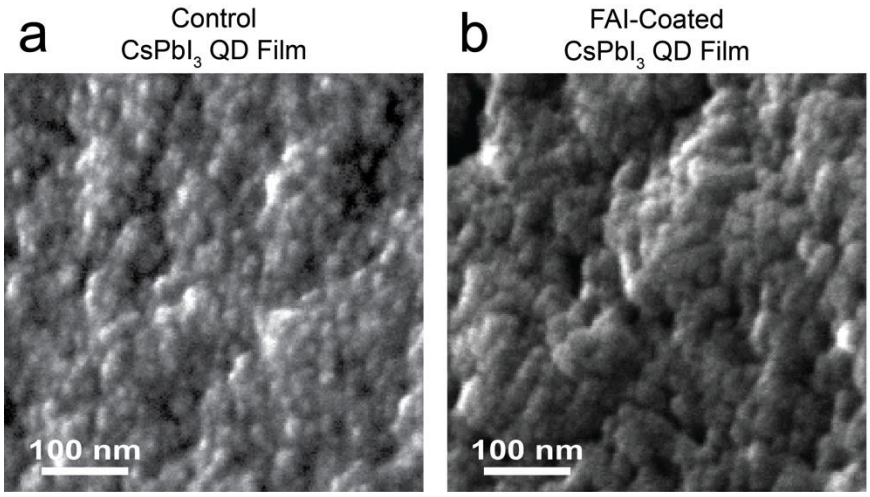

fig. S8. $CsPbI_3$ QD film morphology. SEM micrographs of the surface of the control and FAI-coated QD films show closely-packed assemblies of discrete nanoparticles in both cases.

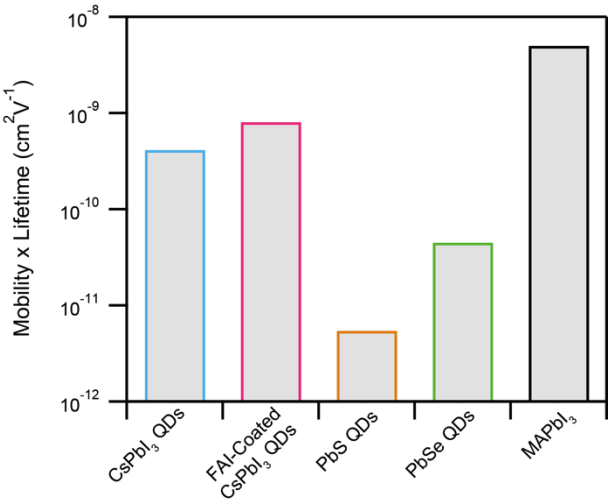

fig. S9. Comparison of terahertz $\mu_s \times \tau$ product. Comparison of the $\mu_s \times \tau$ product calculated from THz spectroscopy for the control $CsPbI_3$ QD and FAI-coated $CsPbI_3$ QD films compared to a PbS QD film, a PbSe QD film, and a $MAPbI_3$ thin film.

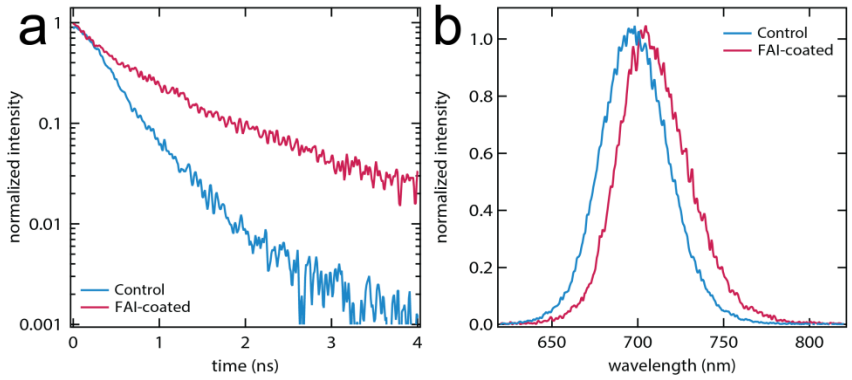

fig. S10. PL lifetime of $CsPbI_3$. Time resolved photoluminescence decay plots for $CsPbI_3$ QD films with (pink) and without (blue) FAI post-treatment.